In-Situ Synthesis of Doped Bio-Graphenes as Effective Metal-Free Catalysts in Removal of Antibiotics: Effect of Natural Precursor on Doping, Morphology, and Catalytic Activity

Maryam Afsharpour *, Lugain Radmanesh , Chuanxi Yang *

Posted Date: 22 August 2023

doi: 10.20944/preprints202308.1387.v1

Keywords: Bio-graphen; Metal-free; Doped; Antibiotic.

Article

In-Situ Synthesis of Doped Bio-Graphenes as Effective Metal-Free Catalysts in Removal of Antibiotics: Effect of Natural Precursor on Doping, Morphology, and Catalytic Activity

Maryam Afsharpour [1,*], Lugain Radmanesh [1] and Chuanxi Yang [2,*]

[1] Department of Inorganic Chemistry, Chemistry & Chemical Engineering Research Center of Iran, 14335-186, Tehran, Iran; afsharpour@ccerci.ac.ir

[2] School of Environmental and Municipal Engineering, Qingdao University of Technology, Qingdao, Shandong, 266520, China: yangchuanxi1989@hotmail.com

* Correspondence: afsharpour@ccerci.ac.ir, yangchuanxi1989@hotmail.com.

Abstract: Wastewater contaminated with antibiotics is a major environmental challenge. We developed here the green synthesis of bio-graphenes by using natural precursors (Xanthan, Chitosan, Boswellia, Tragacanth). The use of these precursors can act as templates to create 3D doped graphene structures with special morphology. Also, this method is a simple method for *in-situ* synthesis of doped graphenes. The elements present in the natural polymers (N) and other elements in the natural composition (P, S) are easily placed in the graphene structure and improve the catalytic activity due to the structural defects, surface charges, increased electron transfers, and the high absorption. In this mechanism, O_2 dissolved in water absorbs onto the positive charged C in doped graphenes to create oxygenated radicals, which enables the degradation of antibiotic molecules. Light irradiation increases the amounts of radicals and rate of antibiotic removal. The results have shown that the hollow cubic Chitosan-derived graphene has shown the best performance due to the doping of N, S, and P. The Boswellia-derived grapheme shows the highest surface area, but lower catalytic performance, which indicates the more effective role of doping in the catalytic activity. The effect of oxygen and light were also studied to accelerate the degradation process.

Keywords: bio-graphen; metal-free; doped; antibiotic

1. Introduction

In recent years, the wastewater contaminated with pharmaceuticals is one of the most important environmental concerns, which have become an emerging environmental challenge [1–4]. Every year, many antibiotics which are used to increase the health quality of humans, release to environment. Since, the conventional wastewater treatment methods used by the pharmaceutical industry are not able to completely remove antibiotics, therefore, the wastewater contains a significant amount of antibiotics. In addition, the unmetabolism antibiotics released by humans and animals has led to the large amounts of antibiotics into municipal and livestock wastewaters. These antibiotics in wastewater lead to the challenges of antibiotic resistance that is a major environmental problem threating the human health and safety of other terrestrial and aquatic organisms [4,5]. Currently, several physical, chemical, and biological technologies have been developed to remove antibiotics from wastewater. Physical methods include filtration, membrane, absorption, coagulation, and sedimentation, which are based on electric attraction, van der Waals forces, gravity, and using physical barriers [6,7]. These methods need post-treatment for accumulated pharmaceutical contaminants. In biological methods, microorganisms are used to break down organic pollutants using cellular processes and convert them into simple materials and biomass [8,9]. These methods in

 doi:10.20944/preprints202308.1387.v1

a traditional ways are also non-effective. Catalytic, photocatalytic, and electrocatalytic processes, ion exchange, and oxidation are the chemical processes used for wastewater treatment [10–13]. Among these methods, advanced oxidation processes (AOPs) are the well-known and effective methods for removal of various organic pollutants such as dyes, antibiotics, pesticides, and, etc [14–20]. Metal oxide semiconductors are the largest group of these catalysts that can fully destroy organic pollutants based on catalytic, photocatalytic, or electrophotocatalytic processes according to the different oxidation mechanism [19–26]. Another category of AOPs catalysts are metal-free catalysts. From this category, we can mention carbon nitrides (g-C_3N_4) [27–29], silicon carbides (SiC) [30], and siligraphenes [31,32]. Although carbon materials were also used to improve the surface area and adsorption, they can be used as an effective oxidation catalyst in the doped forms [33–37]. Kang et al. [33] and Wu et al. [34] reported the degradation of antibiotics in the presence of N-doped graphene for activation of peroxymonosulfate.

In this study, doped graphenes were in-situ synthesized by using natural precursors. The effect of natural precursor on morphology, surface area, doping, and band levels were evaluated here. The doped structures were then tested for degradation of antibiotics via an advanced oxidation mechanism, and different structural parameters were investigated. In this research, only saturated oxygen in water (air bubbling) was used and no oxidants was added to the system. The effect of oxygen and light were also studied to accelerate the degradation process.

2. Results and Discussion

2.1. Characterization of synthesize bio-graphenes

Carbon-based materials which are synthesized from natural materials (biochars or bio-graphenes) are of particular importance due to easy, cheap, and green synthesis method. The use of natural precursors can act as a template and create a structure with special porosity and morphology. Here we have chosen natural gums as precursors. These natural polymers can create a unique polymeric network to produce the 3D graphene structures. The porosity and morphology of these graphenic structures are directly dependent on the natural precursors. Figure 1 shows the SEM images of bio-graphenes synthesized from different natural sources. As can be seen, several morphologies have been created using different natural precursors. Figure 1a shows the hollow sphere structure obtained from natural Xanthan. This compound is produced from fermentation process of single sugers by Xanthomonas campestris bacteria. The EDX results show the N-doped graphene structure for the compound, which is caused by the presence of nitrogen compounds in the original natural composition. Na, K, Ca, and Mg elements have been removed in the acid washing step, which themselves are effective in creating porosity in the structure. Figure 1b shows the hollow cubic structure for bio-graphene derived from natural Chitosan. Chitosan is a linear polysaccharide which made from the chitin shells of shrimp and other crustaceans. The presence of amino groups in the structure of this compound has created a N-doped structure in the obtained graphene. The presence of P and S elements in this structure indicates the presence of compounds containing these elements in the original natural composition, which has led to the creation of N, P, S-doped graphene. Figure 1c presents the SEM image of bio-graphene derived from Boswellia resin. Boswellia is a sticky herbal extract made from the boswellia tree. This resin produces a porous bio-graphene resulting from the 3D network created by this polymer. SEM images of bio-graphenes derived from Tragacanth gum is presented in Figure 1d. Tragacanth is a natural gum obtained from Middle Eastern legume species. As can be seen, this compound shows a layered porous structure in which nitrogen is doped. As can be seen, this bio-graphene (T-BG) shows a layered porous structure in which nitrogen is doped.

Preprints (www.preprints.org) | NOT PEER-REVIEWED | Posted: 22 August 2023 doi:10.20944/preprints202308.1387.v1

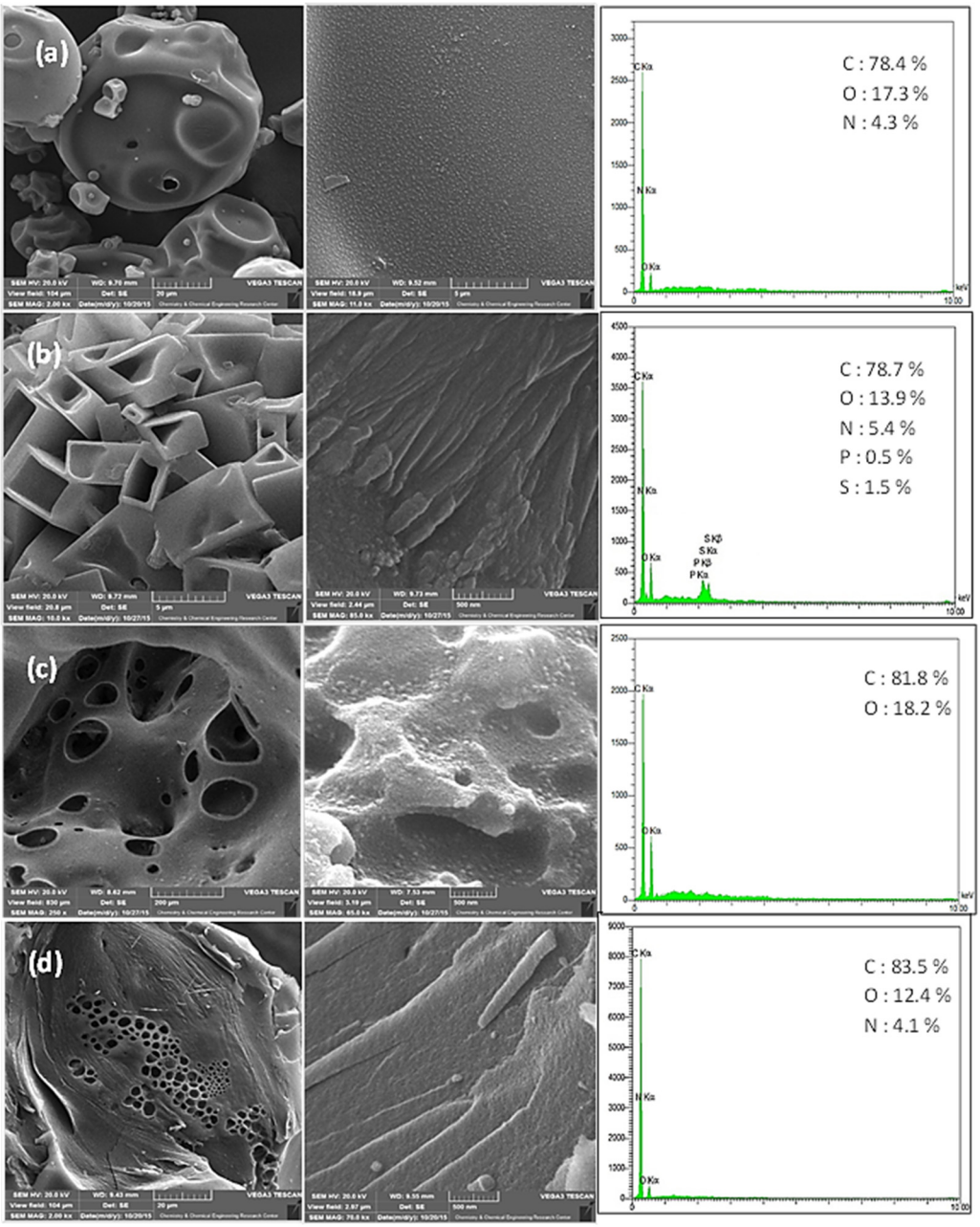

Figure 1. SEM images of (a) X-BG; (b) C-BG; (c) B-BG; and (d) T-BG.

Figure 2 shows the FT-IR spectra of synthesized bio-graphenes. In all samples, the stretching vibrations of the C=C, C-O, and C=O bonds were observed at about 1115, 1630, and 1720 cm^{-1}. Also, the broad band at about 3300-3600 cm^{-1} are related to stretching vibrations of O-H and N-H bonds, and the absorption bands at about 2925 and 2895 cm^{-1} indicate the symmetric and asymmetric C-H vibrations. In X-BG, C-BG, and T-BG samples which shows the N-doping, the C-N absorption bands appeared at 1425 cm^{-1}, and presence of P and S dopants in C-BG sample observed at 895 cm^{-1} and 1080 cm^{-1}, indicating the S-C and P-O bonds in this doped graphene.

Preprints (www.preprints.org) | NOT PEER-REVIEWED | Posted: 22 August 2023 doi:10.20944/preprints202308.1387.v1

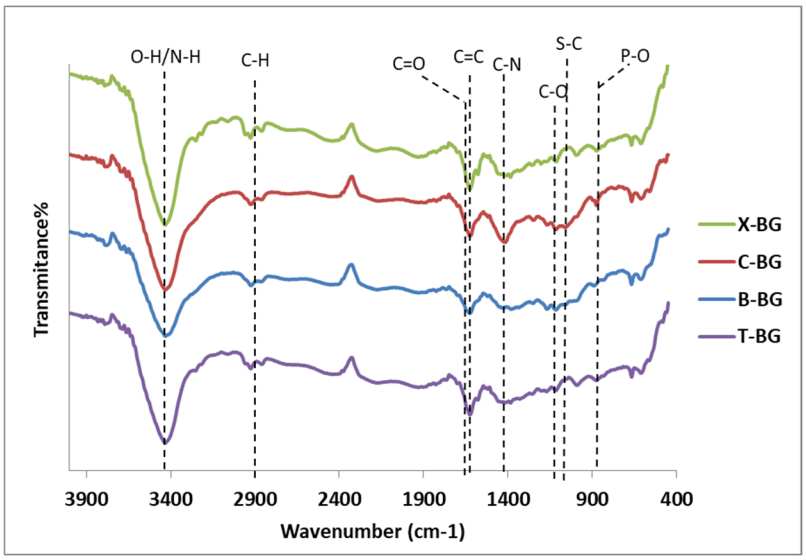

Figure 2. FT-IR spectra of Synthesized bio-graphenes.

Figure 3 shows the Raman spectra of synthesized bio-graphenes. Two characteristic graphene bands of D and G were observed for all samples at about 1584 and 1313 cm^{-1}, respectively. The intensity of D band was increased by increasing the defects in the graphene structure. Doping of heteroatoms increase the degree of disorder and the intensity ratio of D and G bands (I_D/I_G) is increased. Results show that the highest I_D/I_G ratio is related to the C-BG graphene which is derived from Chitosan. It indicates the higher defects in the C-BG graphene structure due to the doping of N, P, and S. The lowest I_D/I_G ratio is related to the B-BG which shows the graphene structure with no element doping.

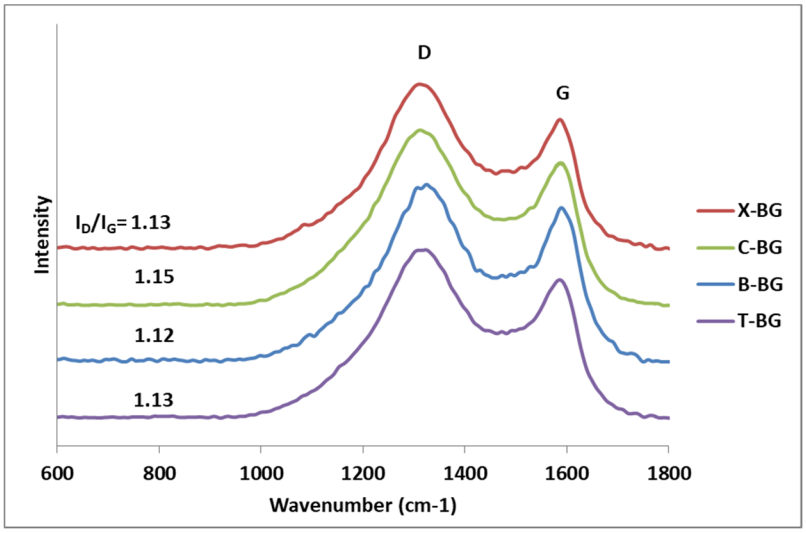

Figure 3. Raman spectra of synthesized bio-graphenes.

To confirm the placement of N, P, and S in the graphene structures, XPS analysis was done (Figure 4). Sample X-BG, C-BG, and T-BG show the doping of nitrogen in the graphene structures. The pyridinic N and pyrrolic N (398.5, and 400.5 eV) are the nitrogen species which are characterized in all samples. The amount of pyridinic N is hogher than pyrrolic N species in X-BG and C-BG samples. In T-BG sample, the pyrrolic N is dominant. Previous results show that these nitrogen species are effective in catalytic oxidative reactions [38–41]. The amounts of nitrogen were measured 4.5, 5.1, and 4 for X-BG, C-BG, and T-BG, respectively which is in agreement with EDX analysis. The presence of P and S in the B-BG structure was also confirmed by XPS analysis (Figure 4b). Results

Preprints (www.preprints.org) | NOT PEER-REVIEWED | Posted: 22 August 2023 doi:10.20944/preprints202308.1387.v1

show the bonding of phosphor with oxygen (P-O) at 134.2 and 134.9 eV and bonding of sulfur with carbon (S-C) and oxygen (C-SO_x-C) at 168.9 eV and 170.6 eV, respectively. The amount of P and S were obtained 0.3 and 1.4, respectively.

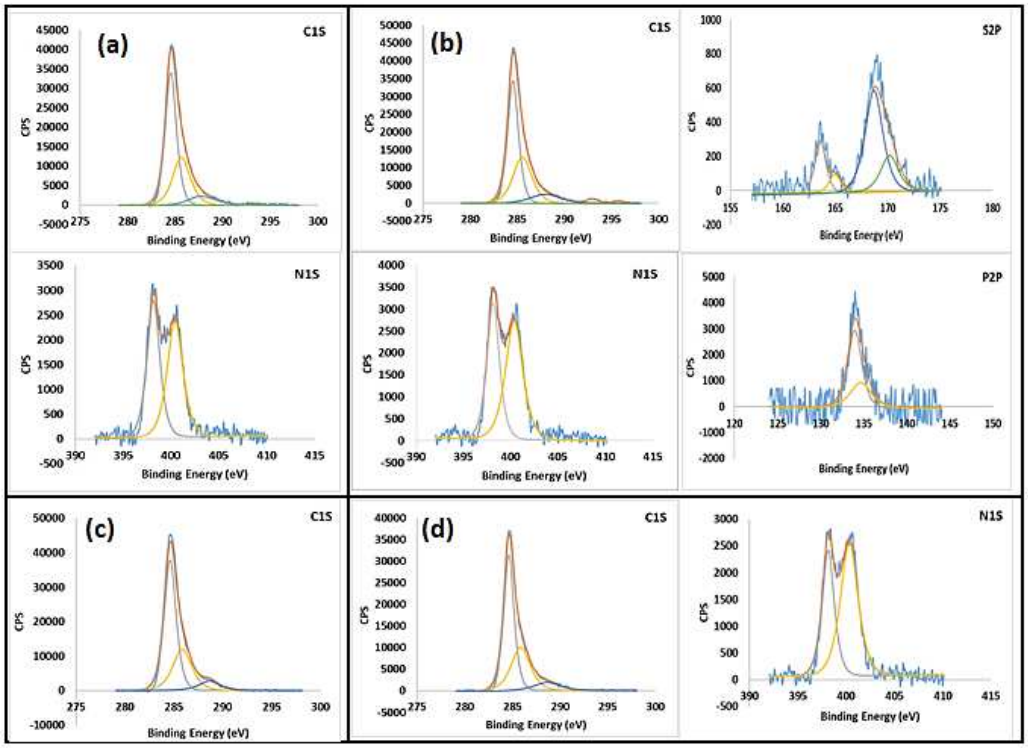

Figure 4. XPS analysis of synthesized bio-graphenes (a) X-BG; (b) C-BG; (c) B-BG; and (d) T-BG.

Since the amount of adsorption is related to the porosity of substrate, the porosities of synthesized bio-graphenes were discussed in Figure 5. The results show the highest surface area for B-BG sample, which is due to its precursor, creating a structure with different pore distribution. After that, the largest surface area is related to C-BG sample, which has the highest amount of dopants, and X-BG and T-BG samples show almost the same surface area. These two samples show more similar nitrogen amounts and morphologies.

2.2. Catalytic Study

In order to investigate the catalytic properties of synthesized bio-graphene, the removal of antibiotics from wastewater was investigated. Tetracycline (TCL), ciprofloxacin (CIP), and amoxicillin (AMX) were tested as the model antibiotics and the removal efficiency of synthesized catalysts were evaluated in the presence of air, oxygen, and light.

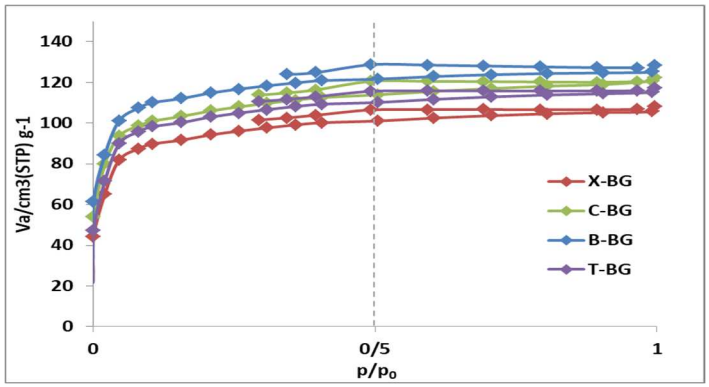

Preprints (www.preprints.org) | NOT PEER-REVIEWED | Posted: 22 August 2023 doi:10.20944/preprints202308.1387.v1

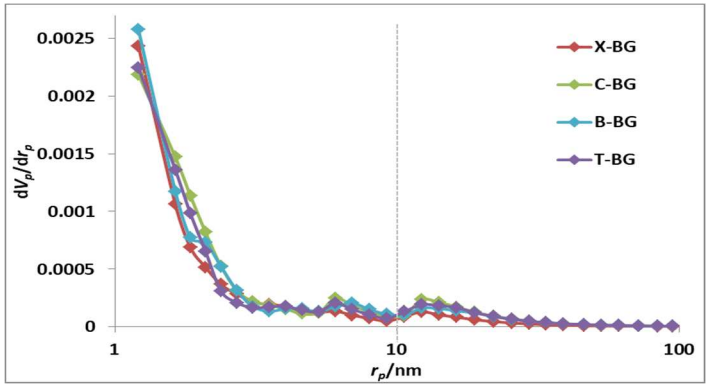

Figure 5. N_2 adsorption/desorption isotherms and pore size distribution curves of synthesized bio-graphenes.

Figure 6a shows the catalytic removal of tetracycline (TCL) using bio-graphenes derived from different natural precursors. As can be seen in the Figure, the highest amount of TCL removal is related to C-BG sample, in which N, P, and S elements are doped, resulting the role of dopants in improving of catalytic properties. X-BG and T-BG samples also show higher catalytic activities than B-BG catalyst, although B-BG has the largest surface area. This result shows that the effect of doping was far greater than the effect of surface area in catalytic activity. X-BG and T-BG samples, which have almost equal amount of nitrogen and surface area and similar morphology, show similar catalytic results.

Figure 6b shows the stability of these catalysts that after 5 runs, only a slight change in their catalytic properties were observed, confirmation the structural stability of these compounds, which is one of the characteristics of a good catalyst.

Figure 6c and d shows the optimization of the catalytic conditions of C-BG in the removal of TCL. The results show that by increasing the amount of catalyst to 15 mg, the catalytic activity increased, but the further increase in the amount of the catalyst only increase the rate of reaction. Figure 6d shows that the best result in the removal of TCL is related to lower concentrations of this antibiotic, by increasing the concentration of the antibiotic, the amount of removal decreases slightly.

Preprints (www.preprints.org) | NOT PEER-REVIEWED | Posted: 22 August 2023 doi:10.20944/preprints202308.1387.v1

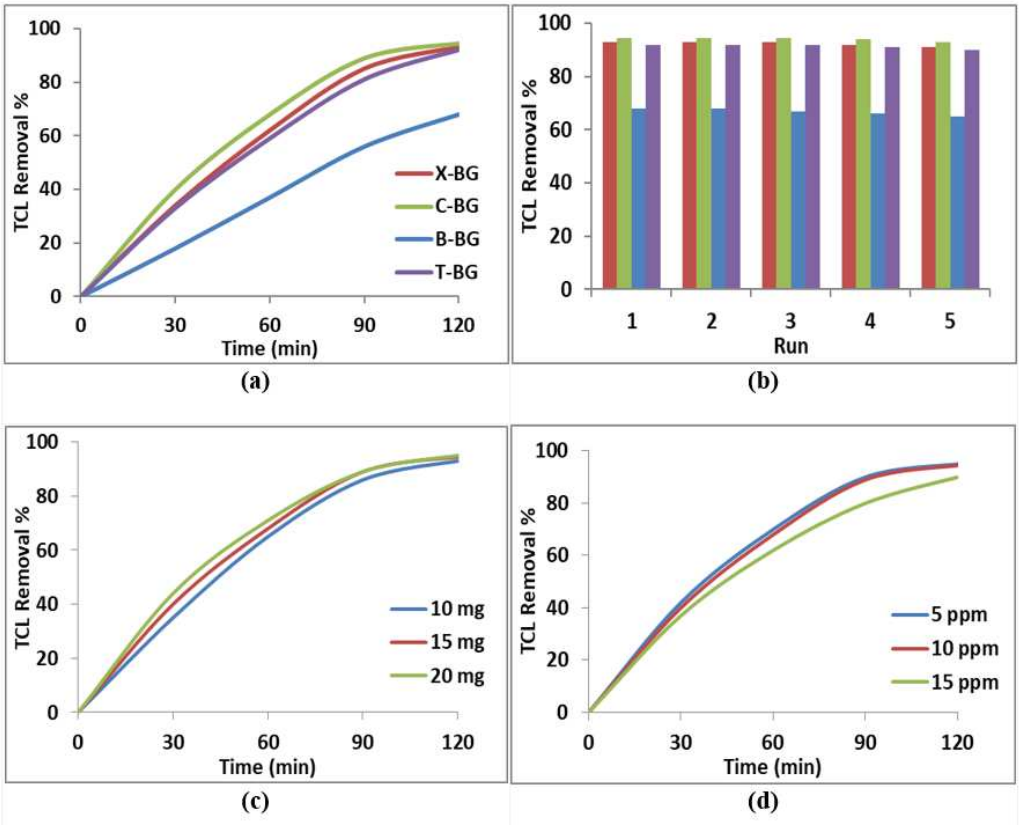

Figure 6. Catalytic efficiency of synthesized bio-graphenes in removal of TCL (a); Recovery of catalysts in TCL removal (b); Effect of different amount of C-BG catalyst (c); and Effect of different TCL concentrations (d).

To investigate the catalytic removal mechanism, the reaction was also performed in the presence of O_2 and light, and the radicals participating in the reaction were identified. Figure 7a shows the results of catalytic activity in different conditions. As can be seen, by using O_2 gas instead of air, the rate of reaction and yield of TCL removal increases, which shows that oxygen is involved in the reaction mechanism. Figure 7b shows the quenching test results. In both conditions, the presence of air and O_2, the formation of oxygenated radicals was observed (Figure 7b). In air condition, hydroxyl ($^{\bullet}OH$) radical is the dominant active specie, while in the presence of O_2, the role of the $^{\bullet}O_2^-$ radical increases. By irradiating light to the system, the rate of reaction and the yield of TCL removal increases (Figure 7a), indicating an increase in the production of oxygenated radicals. According to Figure 7b, the active radical in this system is the $^{\bullet}O_2^-$ radical.

In Figure 7c, the mechanism of TCL removal was displayed. In this mechanism, the oxygen molecules dissolved in water (saturated by air bubbling) adsorb on the positive carbon atoms adjacent to nitrogen atoms [40]. Doping the nitrogen onto the graphene structure create the positive charged carbon atoms which induced by charge polarization of nitrogen atoms. These positive charged C atoms made the active sites to adsorb the oxygen molecules to produce the oxygenated radicals. As shown in Figure 7c, O_2 and H_2O molecules can easily chemisorb on doped graphenes by bonding of O atoms to positive carbon sites. The O-O bond is dissociated and different oxygenated radicals are produced in the presence of water. These radicals can proceed the degradation of TCL via oxidation reaction [16,17,40]. P and S dopants also have the same function as nitrogen. B-BG sample can only remove the TCL via the adsorption mechanism.

To present the efficiency of these doped bio-graphenes to remove the different antibiotics, the removal of ciprofloxacin (CIP) and amoxicillin (AMX) were also investigated (Figure 7d). Results show the good catalytic activity of C-BG in removal of various antibiotics.

Preprints (www.preprints.org) | NOT PEER-REVIEWED | Posted: 22 August 2023 doi:10.20944/preprints202308.1387.v1

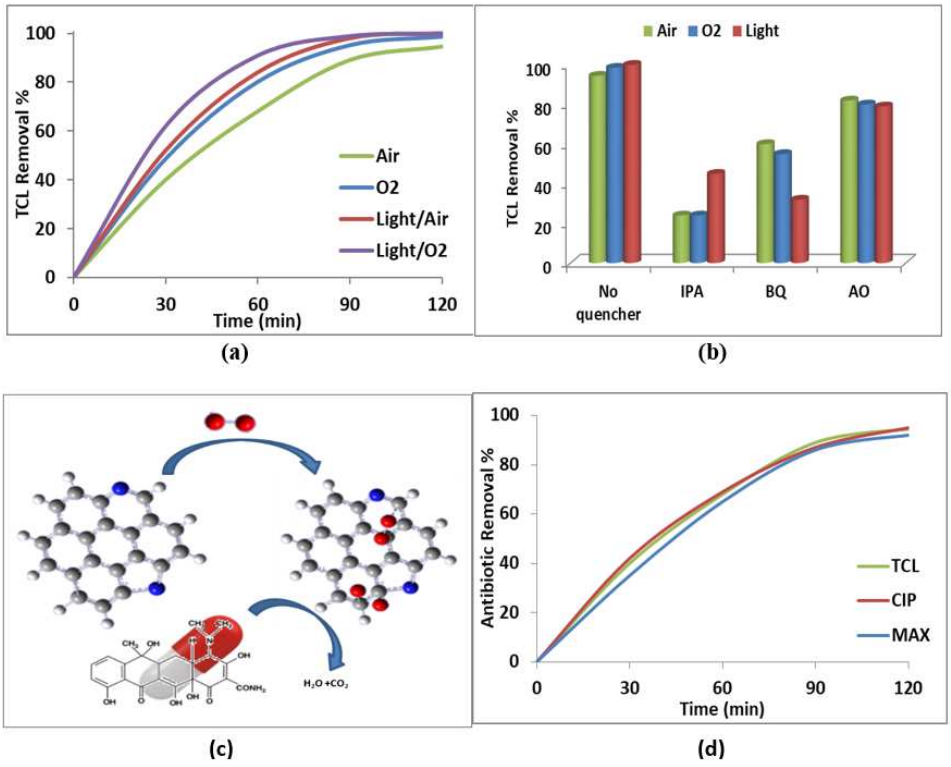

Figure 7. Catalytic performances of C-BG in removal of TCL in presence of air, O2, and light (a); Quenching test in TCL removal in presence of air, O2, and light (b); Mechanism of TCL removal (c); and Catalytic performances of C-BG in removal of different antibiotics (d).

3. Experimental

3.1. Materials and Methods

Natural precursors were used for synthesis of bio-graphenes. Xanthan, Chitosan, Boswellia, and Tragacanth gums were purchased from local shop and used after washing with water to remove the dust. Tetracycline (TCL), ciprofloxacin (CIP), and amoxicillin (AMX) were selected as the model antibiotics to test the removal efficiency of synthesized bio-graphenes.

Scanning electron microscopy with energy dispersive X-ray spectroscopy (SEM/EDX) were used for surface analysis by TESCAN, VEGA3 microscope. FT-IR spectra were taken from Bruker, Vector spectrometer. Raman spectra were obtained from Bruker, Senterra micro-Raman. ESCALAB 250Xi Thermo Scientific system was used for XPS analysis by using a spectrometer with MgKα=1253.6 eV. Photocatalytic tests were measured by a Perkin-Elmer, Lambda-35 UV-Vis spectrometer.

1.2. Synthesis of bio-graphenes

5 g of each natural precursor (Xanthan, Chitosan, Boswellia, or Tragacanth gum) was dissolved in 50 ml water at 50 °C. The solution was stirred until clear gel was obtained. The solutions were filtered to remove the impurities. Then, the obtained gels were dried at 80 °C for 12 h, and the resulting powders were transferred to a crucible and heated at 750 °C with the rate of 5 °/min for 1 h at N_2 atmosphere. The obtained bio-graphenes were washed with diluted HCl to remove the metals (Ca, Mg, K, and Na species). The bio-graphenes were obtained from Xanthan, Chitosan, Boswellia, and Tragacanth gums named X-BG, C-BG, T-BG, and B-BG, respectively.

Preprints (www.preprints.org) | NOT PEER-REVIEWED | Posted: 22 August 2023 doi:10.20944/preprints202308.1387.v1

1.2. Catalytic study

To investigate the performance of synthesized bio-graphenes in the catalytic removal of antibiotics, a certain amount of doped graphenes was added to 10 mL of tetracycline (TCL) solution with different concentrations (5, 10 and 15 ppm). The system was saturated with oxygen by air bubbling during stirring. To optimize the photocatalytic reaction, different amounts of graphene catalyst (10, 15 and 20 mg) were tested for degradation of TCL at pH 2-12. First, all the samples were stirred for 10 min to reach the equilibrium and then removal of TCL was measured in the presence of dissolved oxygen. After every 10 min, TCL concentration was measured by UV-Vis spectroscopy at 357 nm. The TCL removal % was determined using the following equation:

$$\text{Removal \%} = \left[\frac{(C_0 - C_t)}{C_0}\right] * 100\%$$

where C0 and Ct are the initial and equilibrium TCL concentrations, respectively.

In order to investigate the role of oxygen and light, the above process was repeated in the presence of O_2 gas and under visible light irradiation. To investigate the reaction mechanism and determine the active radicals, the quenching tests were done by using 2 Mm of isopropanol (IPA) as the scavenger of hydroxyl radical (•OH), 1,4-benzoquinone (BQ) as the scavenger of superoxide radical anions ($\bullet O_2^-$), and ammonium oxalate (AO) as the hole (h^+) scavenger.

In order to check the ability of the mentioned catalysts to remove all kinds of antibiotics, catalytic tests were also performed for two other antibiotics (ciprofloxacin (CIP), and amoxicillin (AMX)).

Schematic illustration of synthesis procedure and their catalytic properties were displayed in Scheme 1.

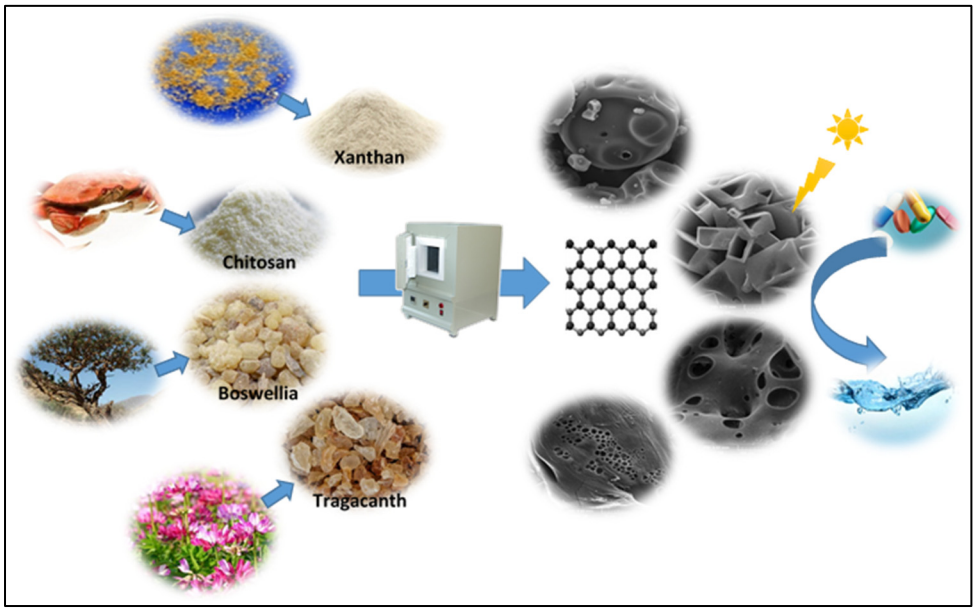

Scheme 1. Schematic illustration of synthesis procedure.

5. Conclusions

In this study, bio-graphenes with different morphology and porosity were synthesized via a green method by using natural precursors (Xanthan, Chitosan, Boswellia, Tragacanth gums). These natural polymers act as templates and create special networks that to form the 3D graphene structure with special morphology. In this method, the elements present in the natural polymers (N) or in the natural composition (P, S) are easily placed in the graphene structure and doped graphenes were synthesized. Doping can improve the catalytic activity due to the structural defects, surface charges, increased electron transfers, and the high absorption. In this mechanism, O2 dissolved in water absorbs onto the positive charged C in doped graphenes to produce the oxygenated radicals, which enables the degradation of antibiotic molecules. Light irradiation increases the amounts of radicals

and rate of antibiotic removal. Oxygen also can accelerate the degradation process via increasing the oxygenated radicals.

Funding: This research received no external funding.

Institutional Review Board Statement: Not applicable.

Informed Consent Statement: Not applicable.

Data Availability Statement: Data is available within the paper. Should any raw data files be needed in another format they are available from the corresponding author upon reasonable request. .

Acknowledgments: Support of this work by Chemistry and Chemical Engineering Research Center of Iran is gratefully acknowledged.

Conflicts of Interest: The authors declare no conflict of interest.

Sample Availability: Samples are available from the authors.

References

1. Larsson, D.J.; de Pedro, C.; Paxeus, N. Effluent from drug manufactures contains extremely high levels of pharmaceuticals, *J. hazard. Mater.* **2007**, *148*, 751-755.
2. Phoon, B.L.; Ong, C.C.; Saheed, M.S.M.; Show, P.L.; Chang, J.S; Ling, T.C.; Lam, S.S.; Juan, J.C. Conventional and emerging technologies for removal of antibiotics from wastewater, *J. Hazard. Mater.* **2020**, *400*, 122961.
3. Ghasemzadeh-mohammadi, V.; Zamani, B.; Afsharpour, M.; Mohammadi, A. Extraction of caffeine and catechins using microwave-assisted and ultrasonic extraction from green tea leaves: an optimization study by the IV-optimal design. *Food Sci. Biotech.* **2017**, *26*, 1281-1290.
4. Homem, V.; Santos, L. Degradation and removal methods of antibiotics from aqueous matrices–a review, *J. environ. Manag.* **2011**, *92*, 2304-2347.
5. Guo, X.; Yan, Z.; Zhang, Y.; Xu, W.; Kong, D.; Shan, Z.; Wang, N. Behavior of antibiotic resistance genes under extremely high-level antibiotic selection pressures in pharmaceutical wastewater treatment plants, *Sci. Total Environ.*, **2018**, *612*, 119-128.
6. Shimizu, Y.; Okuno, Y.-i.; Uryu, K.; Ohtsubo, S.; Watanabe, A. Filtration characteristics of hollow fiber microfiltration membranes used in membrane bioreactor for domestic wastewater treatment, *Water Res.* **1996**, *30*, 2385-2392.
7. Afsharpour, M.; Khomad, E. Synthesis of bio-inspired porous silicon carbides using Cortaderia selloana and Equisetum arvense grasses as remarkable sulfur adsorbents. *Intern. J. Environ. Sci Technol.* **2019**, *16*, 3125–3134.
8. Oberoi, A.S.; Jia, Y.; Zhang, H.; Khanal, S.K.; Lu, H. Insights into the Fate and Removal of Antibiotics in Engineered Biological Treatment Systems: A Critical Review, *Environ. Sci. Technol.* **2019**, *53*, 7234–7264.
9. Hassan, M.; Zhu, G.; Lu, Y.; AL-Falahi,A.H.; Lu, Y.; Huang, Sh.; Wan, Z. Removal of antibiotics from wastewater and its problematic effects on microbial communities by bioelectrochemical Technology: Current knowledge and future perspectives, *Environ. Eng. Res.* **2021**, *26*, 190405.
10. Jiang, F.; Qiu, B.; Sun, D. Advanced degradation of refractory pollutants in incineration leachate by UV/Peroxymonosulfate, *Chem. Eng. J.* **2018**, *349*, 338-346.
11. Gomi, L.S.; Afsharpour, M. Porous MoO_3@SiC hallow nanosphere composite as an efficient oxidative desulfurization catalyst. *Appl. Organometal. Chem.* **2019**, *33*, e4830.
12. Foroughi, M.; Khiadani, M.;, Kakhki, S.; Kholghi, V.; Naderi, Kh.; Yektay, S. Effect of ozonation-based disinfection methods on the removal of antibiotic resistant bacteria and resistance genes (ARB/ARGs) in water and wastewater treatment: a systematic review, *Sci. Total Environ.* **2022**, *811*, 151404.
13. Gomi, L.S.; Afsharpour, M.; Lianos, P. Novel Porous SiO_2@SiC Core-Shell Nanospheres Functionalized with an Amino Hybrid of WO_3 as an Oxidative Desulfurization Catalyst. *J. Indust. Eng. Chem.* **2020**, *89*, 448-457.
14. Hou, J.; Chen, Z.; Gao, J.; Xie, Y.; Li, L.; Qin, S.; Wang, Q.; Mao, D.; Luo, Y. Simultaneous removal of antibiotics and antibiotic resistance genes from pharmaceutical wastewater using the combinations of up-flow anaerobic sludge bed, anoxic-oxic tank, and advanced oxidation technologies, *Water Res.* **2019**, *159*, 511-520.
15. Afsharpour, M.; Darvishi-Farash, S. Novel synthesis of siligraphene/tungstates (g-SiC/AWO) with promoted transportation of photogenerated charge carriers via direct Z-scheme heterojunctions, *Sci. Report.* **2023**, *13*, 10022.

16. Afsharpour, M.; Elyasi, M.; Javadiaan, H.R. A Novel N-Doped Nanoporous Bio-Graphene Synthesized from Pistacia lentiscus Gum and Its Nanocomposite with WO_3 Nanoparticles: Visible-Light-Driven Photocatalytic Activity. *Molecule*. **2021**, *26*, 6569.
17. Gomi, L.S.; Afsharpour, M.; Ghasemzadeh, M.; Lianos, P. Bio-inspired N, S-doped siligraphenes as novel metal-free catalysts for removal of dyes in the dark. *J. Mol. Liquid*. **2019**, *295*, 111657.
18. Afsharpour, M.; Amooee, S. Porous biomorphic silica@ZnO nanohybrids as the effective photocatalysts under visible light, *Environ. Sci. Pollut. Res.* **2022**, *29*, 49784 – 49795.
19. Chen, F.; Yang, Q.; Sun, J.; Yao, F.; Wang, S.; Wang, Y.; Wang, X.; Li, X.; Niu, C.; Wang, D. Enhanced photocatalytic degradation of tetracycline by AgI/BiVO4 heterojunction under visible-light irradiation: mineralization efficiency and mechanism, *ACS appl. Mater.Interface.* **2016**, *8*, 32887-32900.
20. Xu, H.; Jiang, Y.; Yang, X.; Li, F.; Li, A.; Liu, Y.; Zhang, J.; Zhou, Z.; Ni, L. Fabricating carbon quantum dots doped $ZnIn_2S_4$ nanoflower composites with broad spectrum and enhanced photocatalytic Tetracycline hydrochloride degradation, *Mater. Res. Bull*. **2018**, *97*, 158-168.
21. Wang, H.; Yao, H.; Pei, J.; Liu, F.; Li, D. Photodegradation of tetracycline antibiotics in aqueous solution by UV/ZnO, *Desalin. Water Treatment*, **2016**, *57*, 19981-19987.
22. Tang, X.; Wang, Z.; Wang, Y. Visible active N-doped TiO_2/reduced graphene oxide for the degradation of tetracycline hydrochloride, *Chem. Phys. Lett.* **2018**, *691*, 408-414.
23. Wang, H.; Ye, Z.; Liu, C.; Li, J.; Zhou, M.; Guan, Q.; Lv, P.; Huo, P.; Yan, Y. Visible light driven Ag/Ag_3PO_4/AC photocatalyst with highly enhanced photodegradation of tetracycline antibiotics, *Appl. Surface Sci.* **2015**, *353*, 391-399.
24. Ma, N.; Xu, J.; Bian, Z.; Yang, Y.; Zhang, L.; Wang, H. $BiVO_4$ plate with Fe and Ni oxyhydroxide cocatalysts for the photodegradation of sulfadimethoxine antibiotics under visible-light irradiation, *Chem. Eng. J.* **2020**, *389*, 123426.
25. Rana, A.; Kumar, A.; Sharma, G.; Naushad, M.; Bathula, Ch.; Stadler, F.J. Pharmaceutical pollutant as sacrificial agent for sustainable synergistic water treatment and hydrogen production via novel Z- scheme $Bi_7O_9I_3$/B_4C heterojunction photocatalysts, *J. Mol. Liquid*. **2021**, *343*, 17652.
26. Ivan, R.; Popescu, C.; Antohe, V.A.; Antohe, S.; Negrila, C.; Logofatu, C.; del Pino, A.P.; György, E. Iron oxide/hydroxide–nitrogen doped graphene-like visible-light active photocatalytic layers for antibiotics removal from wastewater, *Sci. Report*. **2023**, *13*, 2740.
27. Song, Y.; Tian, J.; Gao, S.; Shao, P.; Qi, J.; Cui, F. Photodegradation of sulfonamides by gC_3N_4 under visible light irradiation: effectiveness, mechanism and pathways, *Appl. Catal. B: Environ*. **2017**, *210*, 88-96.
28. Wang, Y.; Wang, F.; Feng, Y.; Xie, Z.; Zhang, Q.; Jin, X.; Liu, H.; Liu, Y.; Lv, W.; Liu, G. Facile synthesis of carbon quantum dots loaded with mesoporous gC_3N_4 for synergistic absorption and visible light photodegradation of fluoroquinolone antibiotics, *Dalton Trans.* **2018**, *47*, 1284-1293.
29. Li, C.; Sun, Z.; Huang, W.; Zheng, S. Facile synthesis of g-C_3N_4/montmorillonite composite with enhanced visible light photodegradation of rhodamine B and tetracycline, *J.Taiwan Inst. Chem. Eng*. **2016**, 66, 363-371.
30. Zhu, H.; Yang, B.; Yang, j.; Yuan, Y.; Zhang, J. Persulfate-enhanced degradation of ciprofloxacin with SiC/g-C_3N_4 photocatalyst under visible light irradiation, *Chemosphere.* **2021**, *276*, 130217.
31. Afsharpour, M.; Behtooei, H.R.; Shakiba, M.; Martí, V. Novel N,P,S co-doped graphenic SiC layers (g-SiC) in visible-light photodegradation of antibiotics and inactivating the bacteria. *Process Saf. Environ. Protect*. **2022**, *166*, 704-717.
32. Darvishi-Farash, S.; Afsharpour, M.; Heidarian, J. Novel siligraphene/g-C_3N_4 composites with enhanced visible light photocatalytic degradations of dyes and drugs. *Environ. Sci. Pollut. Res.* **2021**, *28*, 5938–5952.
33. Kang, J.; Zhou, L.; Duan, X.; Sun, H.; Wang, Sh. Catalytic degradation of antibiotics by metal-free catalysis over nitrogen-doped grapheme, *Catal. Today*. **2020**, *357*, 341-349.
34. Wu, N.; Zhang, X.; Zhang, X.; Yang, K.; Li, Y. Simultaneous degradation of trace antibiotics in water by adsorption and catalytic oxidation induced by N-doped reduced graphene oxide (N-rGO): synergistic mechanism, *Mater. Res. Express* **2022**, *9*, 065601.
35. Siddiqui, A.S.; Ahmad, M.A.; Nawaz, M.H.; Hayat, A.; Nasir, M. Nitrogen-doped graphene oxide as a catalyst for the oxidation of Rhodamine B by hydrogen peroxide: application to a sensitive fluorometric assay for hydrogen peroxide, *Microchim. Acta*. **2020**, *187*, 47.
36. Duan, X.; O'Donnell, K.; Sun, H.; Wang, Y.; Wang, Sh. Sulfur and Nitrogen Co-Doped Graphene for Metal-Free Catalytic Oxidation Reactions, *Small*. **2015**, *11*, 3036-3044.
37. Long, J.; Xie, X.; Xu, J.; Gu, Q.; Chen, L; Wang, X. Nitrogen-Doped Graphene Nanosheets as Metal-Free Catalysts for Aerobic Selective Oxidation of Benzylic Alcohols, *ACS Catal*. **2012**, *2*, 622−631.
38. Luo, E.; Xiao, M.; Ge, J.; Liu, Ch.; Xing, W. Selectively doping pyridinic and pyrrolic nitrogen into a 3D porous carbon matrix through template-induced edge engineering: enhanced catalytic activity towards the oxygen reduction reaction, *J. Mater. Chem. A*. **2017**, *5*, 21709-21714.
39. Wang, X.X.; Zou, B.; Du, X.X.; Wang, J.N. N-doped carbon nanocages with high catalytic activity and durability for oxygen reduction, *J. Mater. Chem. A*, **2015,** *3*, 12427-12435.

40. Afsharpour, M.; Gomi, L.S.; Elyasi, M. Novel metal-free N-doped bio-graphenes and their MoO_3 bifunctional catalysts for ultra-deep oxidative desulfurization of heavy fuel, *Separ. Purif. Technol*. **2021**, *274*, 119014.
41. 41.Miao,. H.; Li, Sh.; Wang, Zh.; Sun, Sh.; Kuang, M.; Liu, Zh.; Yuan, J. Enhancing the pyridinic N content of Nitrogen-doped graphene and improving its catalytic activity for oxygen reduction reaction, *Intern. J. Hydrogen Energy*. **2017**, *42*, 28298-28308.